Precision Mechanics & Digital Fabrication
https://www.acadlore.com/journals/PMDF

Mechanical Characterization and Constrained Recovery Behavior of Domestically Produced Fe-Mn-Si Shape Memory Alloys for Structural Strengthening

Honglei Ma, Yifeng Zheng*

College of Construction Engineering, Jilin University, 130012 Changchun, China

* Correspondence: Yifeng Zheng (zhengyf@jlu.edu.cn)

Received: 06-17-2025 **Revised:** 07-31-2025 **Accepted:** 08-12-2025

Citation: H. L. Ma, and Y. F. Zheng, "Mechanical characterization and constrained recovery behavior of domestically produced Fe-Mn-Si shape memory alloys for structural strengthening," *Precis. Mech. Digit. Fabr.*, vol. 2, no. 3, pp. 162–171, 2025. https://doi.org/10.56578/pmdf020303.

Abstract: The fundamental mechanical properties and constrained recovery behavior of two domestically produced Fe-Mn-Si shape memory alloys (SMAs) (Fe-16.86Mn-4.5Si-10.3Cr-5.29Ni-0.08C and Fe-17.6Mn-4.5Si-3.22Cr-2.96Ni-0.28C-1.45V) were investigated with specific reference to their potential application in bridge strengthening. Uniaxial tensile tests, differential scanning calorimetry, and thermal expansion measurements were conducted to determine the elastic modulus, transformation stress, transformation temperatures, and thermal expansion characteristics. The alloy containing vanadium exhibited a higher elastic modulus and a higher transformation stress than the vanadium-free alloy. In addition, the presence of vanadium significantly reduced the width of the transformation temperature interval, which is advantageous for temperature control during practical activation. Constrained recovery tests showed that the recovery stress increased with increasing activation temperature and reached a maximum at a pre-strain of approximately 6%. The level of pre-applied stress had only a minor effect on the final recovery stress, indicating a stable and controllable recovery behavior under engineering conditions. These results provide both experimental data and a mechanical basis for the use of domestically produced Fe-Mn-Si shape memory alloys in the active strengthening of civil engineering structures.

Keywords: Shape memory alloys; Fe-SMAs; Mechanical properties; Constrained recovery performance; Structural strengthening

1 Introduction

As of 2024, more than 300,000 bridges in China have been in service for over 20 years. Most of these aging bridges struggle to meet the growing traffic demands due to multiple factors, including concrete deterioration, steel corrosion, relatively low original design load standards, insufficient construction quality, and a lack of long-term maintenance. With continuously increasing traffic volume and frequent overloaded vehicles, common structural issues such as crack propagation and excessive deflection have emerged in these bridges [1]. Therefore, strengthening and rehabilitating existing aging bridges has become an urgent engineering task, aimed at inhibiting structural deformation, retarding crack development, extending service life, and ensuring safe traffic capacity.

Traditional bridge strengthening methods primarily include section enlargement, externally bonded steel plates, and external prestressing [2]. Although the section enlargement method offers clear mechanical behavior, simple construction, and low cost, it involves prolonged wet-process work, necessitates traffic interruption, and increases structural self-weight while reducing under-clearance. The method of externally bonded steel plates allows for rapid construction and causes minimal damage to the original structure. However, the anti-corrosion treatment for the steel plates and anchors increases long-term maintenance costs, and the long-term durability of the adhesive layer is difficult to guarantee. External prestressing can fully utilize the properties of high-strength materials and mitigate strain lag issues. Nonetheless, it suffers from complex construction techniques and relatively high long-term maintenance costs [3]. Consequently, the search for novel strengthening materials and technologies that are efficient, durable, and convenient for construction has become a crucial research direction in bridge engineering.

Since their emergence in the 1940s, Fiber-Reinforced Polymer (FRP) composites have found extensive applications in various fields such as aerospace, marine, and automotive industries [4]. In recent years, owing to their advantages of

being lightweight, high-strength, and corrosion-resistant, FRPs have been widely adopted as a novel civil engineering material for strengthening and repairing reinforced concrete and steel structures. Among various techniques, externally bonded FRP has been particularly favored [5–7]. However, externally bonded FRP is inherently a "passive" strengthening technique, meaning its high-strength characteristics are often underutilized in practical engineering. To address this limitation, researchers have attempted to apply prestress to FRP to achieve "active" strengthening [8, 9]. However, this method requires complex tensioning and anchoring equipment, sufficient operational space, and is constrained by on-site construction conditions, all of which limit its widespread application in practice [10, 11]. Therefore, developing an efficient and straightforward active strengthening technology is of significant importance for enhancing the effectiveness of bridge strengthening.

Shape Memory Alloys (SMAs) are a class of SMAsrt materials possessing shape memory effect and superelasticity, which have demonstrated promising application prospects in the field of structural strengthening in recent years [12, 13]. Utilizing the shape memory effect of SMAs, prestress can be actively introduced into structures, significantly enhancing both the load-bearing capacity and serviceability of the strengthened members [14]. Currently, Iron-based SMAs (Fe-SMAs) have gradually become a research focus due to their advantages of relatively low cost, good workability, and high strength [15–17]. Previous studies have applied Fe-SMAs to various scenarios, such as shear strengthening of concrete bridges, fatigue repair of steel truss bridges, and load capacity enhancement of industrial buildings [12, 18]. However, the Fe-SMAs materials currently in widespread use are predominantly sourced from the Swiss Federal Laboratories for Materials Science and Technology (EMPA). Research on domestically produced Fe-SMAs remains insufficient, leaving their fundamental mechanical properties, recovery performance, and engineering applicability unclear. Therefore, this study focuses on two types of domestically produced Fe-Mn-Si-SMAs. Through systematic experimental investigation, it aims to reveal their fundamental mechanical properties and constrained recovery performance, thereby providing theoretical basis and technical support for promoting the application of domestic Fe-SMAs in civil engineering strengthening.

The two Fe-Mn-Si alloys investigated in this study (Fe-16.86Mn-4.5Si-10.3Cr-5.29Ni-0.08C and Fe-17.6Mn-4.5Si-3.22Cr-2.96Ni-0.28C-1.45V) are experimental materials prepared by a domestic partner through processes including vacuum melting and hot rolling. Their composition design references the classic EMPA Fe-17Mn-5Si-10Cr-4Ni-1(V, C) system but has been optimized considering domestic resource availability and processing conditions. Currently, such domestic Fe-SMAs are still in the stage of laboratory research and pilot engineering applications. They possess stable pilot-scale production capability; however, large-scale commercial application cases remain scarce. The work presented in this paper aims to systematically evaluate their fundamental properties, thereby providing foundational data to advance the engineering application of domestic Fe-SMAs.

This paper first introduces the research background and development status of Fe-SMAs, which provides a theoretical basis for the subsequent experimental design. Then, via uniaxial tensile tests, differential scanning calorimetry (DSC), and thermal expansion coefficient measurements, we systematically characterize the elastic modulus, transformation stress, transformation temperatures, and thermal expansion behavior of two domestic Fe-SMAs.

Finally, constrained recovery tests are conducted to investigate the influences of pre-strain level and recovery temperature on the recovery stress of Fe-SMAs, aiming to comprehensively evaluate their engineering feasibility as active strengthening materials.

2 Study on the Fundamental Mechanical Properties of Fe-SMAs Materials

To elucidate the fundamental mechanical properties of domestic Fe-SMAs, this chapter presents uniaxial tensile tests, transformation temperature measurements, and thermal expansion coefficient determinations conducted on two types of Fe-SMAs specimens with different compositions. A systematic analysis of their elastic modulus, transformation stress, transformation temperatures, and thermal expansion behavior is provided.

2.1 SMAs Material Composition and Specimen Preparation

Two types of Fe-SMAs materials were selected for this study. Their chemical compositions are Fe-16.86Mn-4.5Si-10.3Cr-5.29Ni-0.08C (hereafter referred to as "V-free Fe-SMAs") and Fe-17.6Mn-4.5Si-3.22Cr-2.96Ni-0.28C-1.45V (hereafter referred to as "V-added Fe-SMAs"). The raw materials were melted in a vacuum medium-frequency induction furnace and then cast into ingots. Subsequently, the ingots underwent solution treatment at 1200℃ for 24 hours, followed by hot rolling to form slabs. Specimens were machined along the rolling direction using wire electrical discharge machining (wire-EDM), with final dimensions of 125 mm (length) × 5 mm (width) × 1.0 mm (thickness). The geometry and appearance of the tensile specimens are shown in Figure 1. Prior to testing, all specimens were heated at 500℃ for 15 minutes to relieve machining-induced residual stresses. For each test condition, three parallel specimens were used. The data presented in this paper are the average values obtained from these multiple tests.

(a) (b)

Figure 1. Tensile specimens of the shape memory alloys (SMAs) used in the tests: (a) V-added Fe-SMAs specimen; (b) V-free Fe-SMAs specimen

2.2 Uniaxial Tensile Tests of Fe-SMAs Materials

Uniaxial tensile tests were performed on a 100 kN electro-servo hydraulic universal testing machine under displacement control at a rate of 2 mm/min, as shown in Figure 2. The load cell and displacement controller had accuracies of ± 0.5% FS and ± 0.01 mm, respectively. The test results showed that the V-free Fe-SMAs specimen had an elastic modulus of 187.9 GPa and a transformation stress (defined as the stress at 0.2% residual strain [19]) of 427.3 MPa. In comparison, the V-added Fe-SMAs specimen exhibited a higher elastic modulus of 196.7 GPa and a transformation stress of 510.1 MPa. The stress-strain curves indicated that both materials exhibited no distinct yield plateau. Their deformation process comprised three stages: the elastic stage, the transformation stage, and the plastic slip stage.

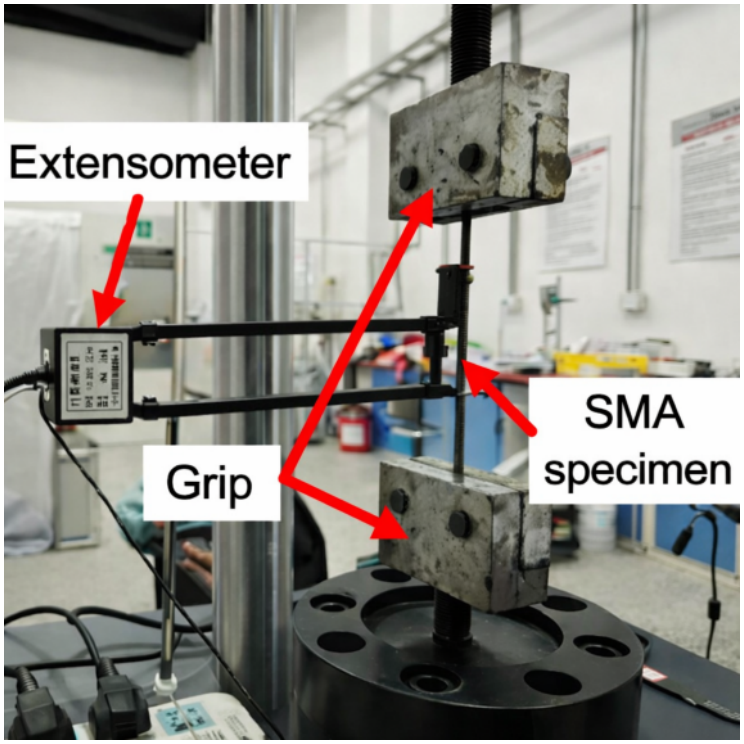

Figure 2. Uniaxial tensile test experimental graph

2.3 Determination of Transformation Temperatures for Fe-SMAs

Techniques commonly used to study the crystalline phase transformation behavior of shape memory alloys include DSC, electrical resistance scanning (ERS), and bend and free recovery (BFR) methods [20]. In this study, the transformation temperatures of the specimens were determined using DSC, with the experimental setup shown in Figure 3. The DSC measurements were conducted with a temperature accuracy of ±0.1°C, a heat flow accuracy of $\pm 1\mu$W, over a temperature range from -150℃ to 500℃, at a heating/cooling rate of 10℃/min. The results revealed that for the V-added Fe-SMAs, the martensite transformation start (M_s) and finish (M_f) temperatures were 33.9℃ and -28.8℃, respectively, while the austenite transformation start (A_s) and finish (A_f) temperatures were 358.5℃ and 432.2℃, respectively. For the V-free Fe-SMAs, the corresponding temperatures were M_s = 16.5℃, M_f = -1.1℃, A_s = 401.7℃, and A_f = 430.6℃. The addition of vanadium significantly lowered both the martensitic and austenitic transformation temperatures. This reduction is beneficial for controlling the activation temperature and enhancing material stability in engineering applications.

Figure 3. The differential scanning calorimetry (DSC) apparatus used for transformation temperature measurements

2.4 Coefficient of Thermal Expansion of Fe-SMAs Materials

The coefficient of thermal expansion (CTE) of the Fe-SMAs specimens was measured within the temperature range of 30℃ to 400℃, using the same testing machine described in Section 2.2. Temperature was monitored using a K-type thermocouple with an accuracy of ± 0.5℃. The results indicated that for both materials, the strain exhibited an approximately linear relationship with temperature during heating. The measured CTE values were 1.33×10^{-5}℃$^{-1}$ for the V-free Fe-SMAs and 1.37×10^{-5}℃$^{-1}$ for the V -added Fe -SMAs. The close proximity of these values suggests that the addition of vanadium has a limited influence on the thermal expansion behavior.

3 Constrained Recovery Performance of Fe-SMAs Materials

The recovery performance of Fe-SMAs forms the foundation for their application in active structural strengthening. This chapter systematically investigates the effects of pre-strain level, recovery temperature, thermomechanical training, solution treatment, hot-rolling process, and pre-applied stress on the recovery stress of Fe-SMAs through constrained recovery tests.

3.1 Experimental Methodology for Recovery Performance of Fe-SMAs

The specimens were first pre-tensioned at a rate of 2 mm/min and then unloaded to introduce a predetermined pre-strain. Subsequently, they were fixed in the grips of the testing machine. Heating was applied using a mica heating plate, with the temperature controlled by a regulator with an accuracy of ±1℃. The heating rate was set at 2℃/min. After reaching the target temperature, the specimens were allowed to cool naturally. Throughout the test, the grip displacement was held constant. The stress and temperature variations of the specimen were monitored in real time using a load cell and a thermocouple, respectively.

3.2 Influence of Heating Temperature on the Recovery Performance of Fe-SMAs

Constrained recovery tests were conducted on V-free Fe-SMAs specimens (with 5% pre-strain) at temperatures of 180℃, 300℃, and 350℃, as shown in Figure 4. The results showed that the maximum recovery stress increased progressively with the activation temperature, reaching values of 180.1 MPa, 284.1 MPa, and 310.6 MPa, respectively. During the initial heating stage, the recovery stress exhibited a slight decrease due to thermal expansion. Subsequently, it rose rapidly driven by the phase transformation. As the transformation neared completion, a decreasing trend reappeared, dominated again by thermal expansion. During the cooling phase, the stress increased further owing to thermal contraction.

Similar tests were performed on V-added Fe-SMAs specimens (5% pre-strain) over a temperature range of 180℃ to 400℃. A similar trend of increasing recovery stress with temperature was observed, as illustrated in Figure 5. However, due to the lowered transformation temperatures caused by vanadium addition, the V-added specimens generated higher recovery stresses at identical activation temperatures, with the maximum recovery stresses quantified in Figure 6. Moreover, the stress drop induced by thermal expansion was less pronounced in these specimens.

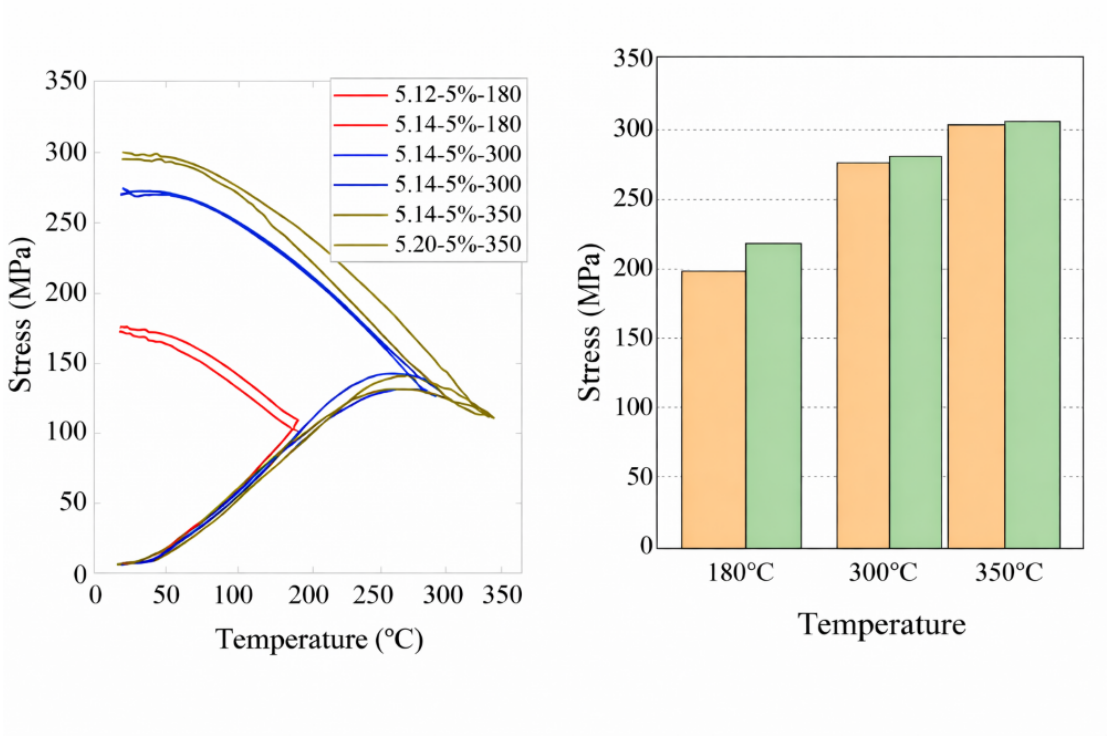

Figure 4. Temperature-stress curves of the V-free Fe-SMAs specimen at different recovery temperatures

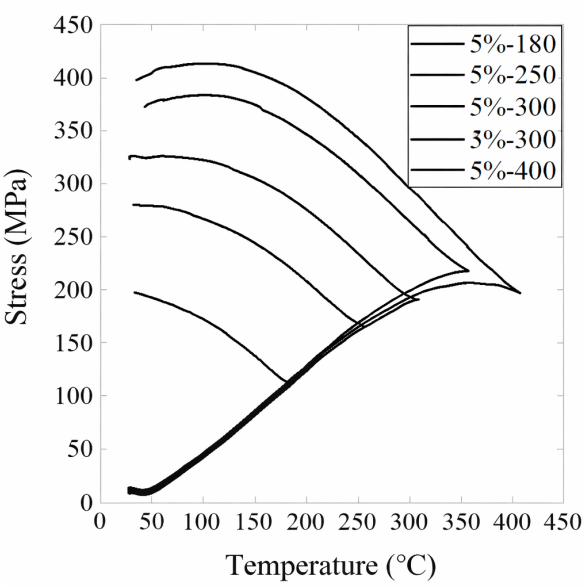

Figure 5. Stress-temperature curves of the V-added Fe-SMAs specimen at different recovery temperatures

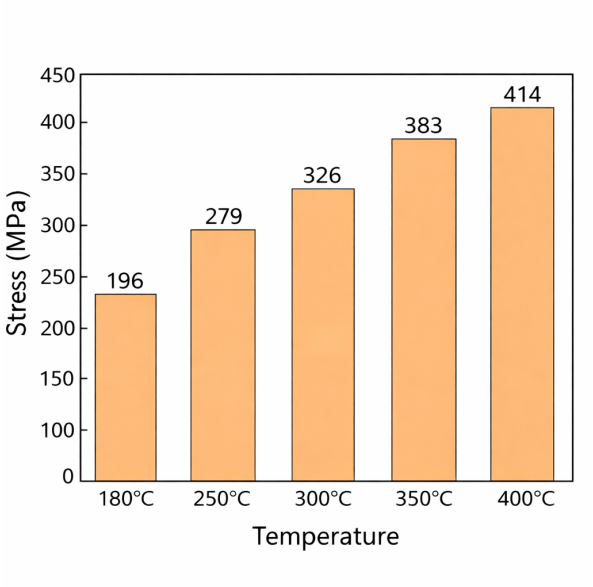

Figure 6. Maximum recovery stress of the V-added Fe-SMAs specimen at different recovery temperatures

3.3 Effect of Pre-strain Level on Recovery Performance

The influence of pre-strain level on the recovery stress of both V-free and V-added Fe-SMAs at activation temperatures of 180℃ and 350℃ is comprehensively shown in Figures 7–14.

The experimental results indicate that, at a constant activation temperature, the recovery stress of Fe-SMAs increases with the pre-strain level, but an optimal pre-strain value exists. For the V-free Fe-SMAs at an activation temperature of 350℃, the recovery stress reached its maximum value of 301.8 MPa at 6% pre-strain. A further increase in pre-strain to 8% led to a slight decrease in recovery stress. Similarly, for the V-added Fe-SMAs at 350℃, the maximum recovery stress of 361.8 MPa was achieved at 6% pre-strain, beyond which the recovery stress showed a declining trend. This suggests that an appropriate pre-strain can fully induce the martensitic transformation, whereas

excessive pre-strain may introduce irreversible plastic deformation, thereby reducing the recovery effectiveness.

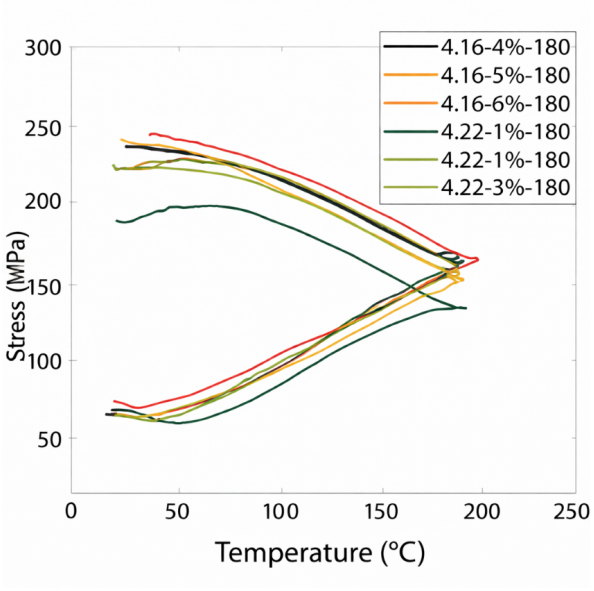

Figure 7. Stress-temperature curves of the V-free Fe-SMAs specimen at different pre-strain levels (recovery at 180℃)

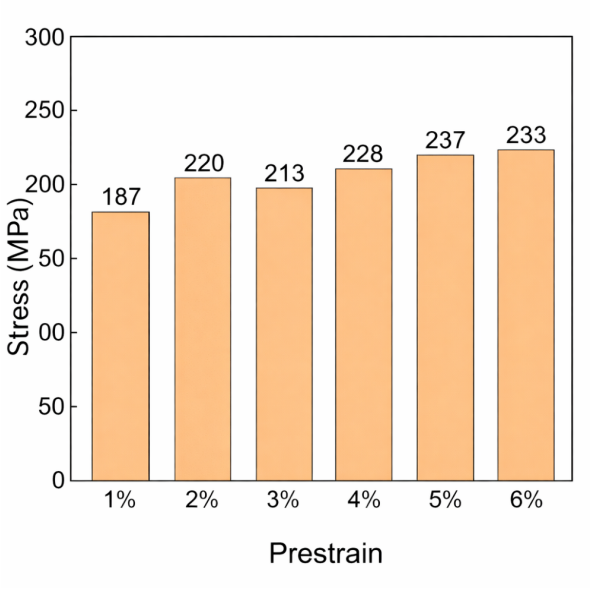

Figure 8. Maximum recovery stress of the V-free Fe-SMAs specimen at different pre-strain levels (recovery at 180℃)

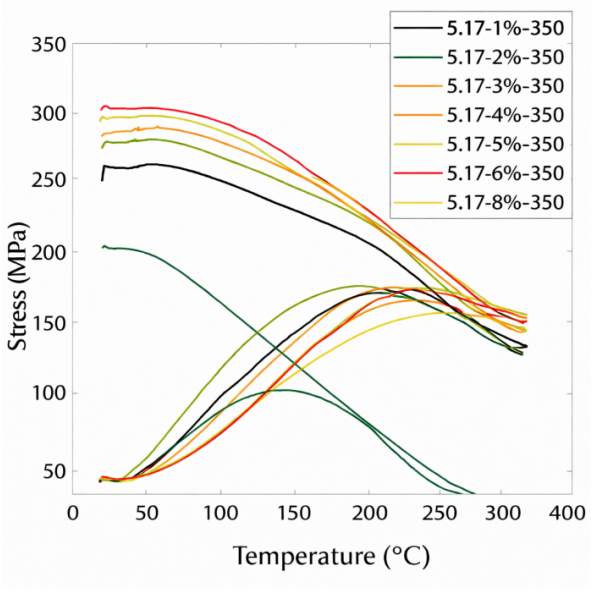

Figure 9. Stress-temperature curves of the V-free Fe-SMAs at different pre-strain levels (recovery at 350℃)

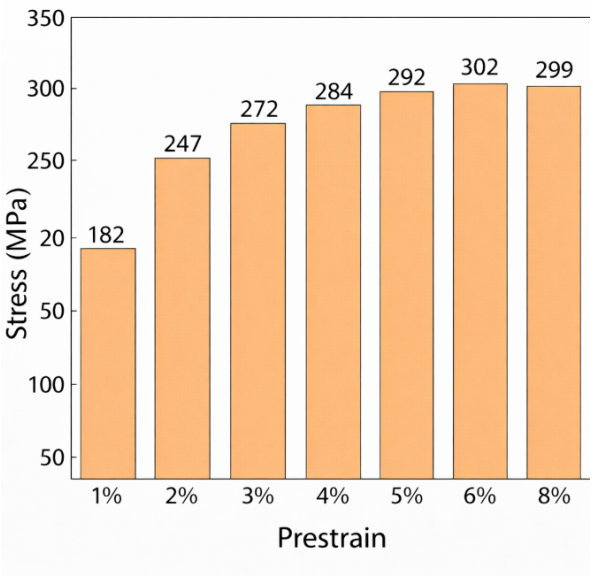

Figure 10. Maximum recovery stress of the V-free Fe-SMAs at different pre-strain levels (recovery at 350℃)

3.4 Relationship Between Transformation Temperatures and Recovery Stress

The experimental results from this study demonstrate a close correlation between the recovery stress of Fe-SMAs and their transformation temperature intervals. The V-added Fe-SMAs possesses lower A_s and A_f temperatures (358.5℃ and 432.2℃, respectively). This implies that at an identical activation temperature, the V-added material is closer to, or already within, the completion stage of the austenitic transformation.

Consequently, it yields more complete, higher-magnitude recovery stresses. By contrast, the V-free Fe-SMAs has a higher A_s: at the same temperature, its weaker phase transformation driving force leads to lower recovery

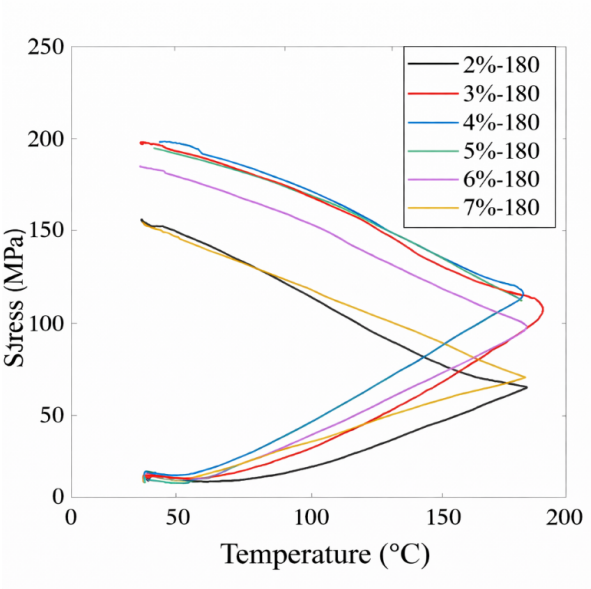

Figure 11. Stress-temperature curves of the V-added Fe-SMAs at different pre-strain levels (recovery at 180℃)

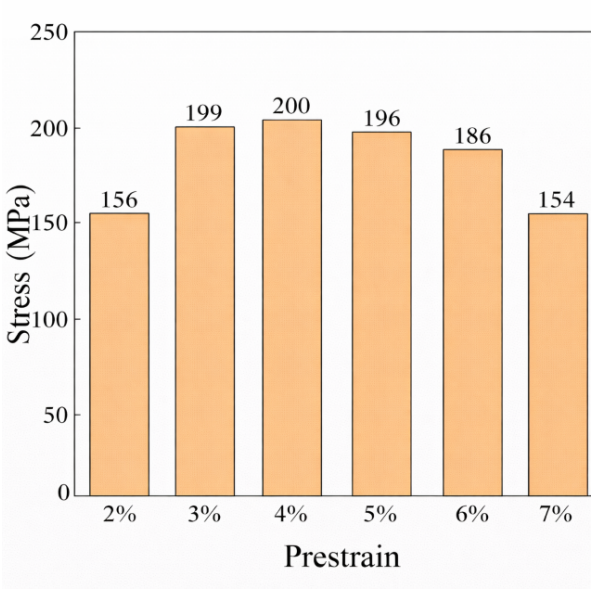

Figure 12. Maximum recovery stress of the V-added Fe-SMAs at different pre-strain levels (recovery at 180℃)

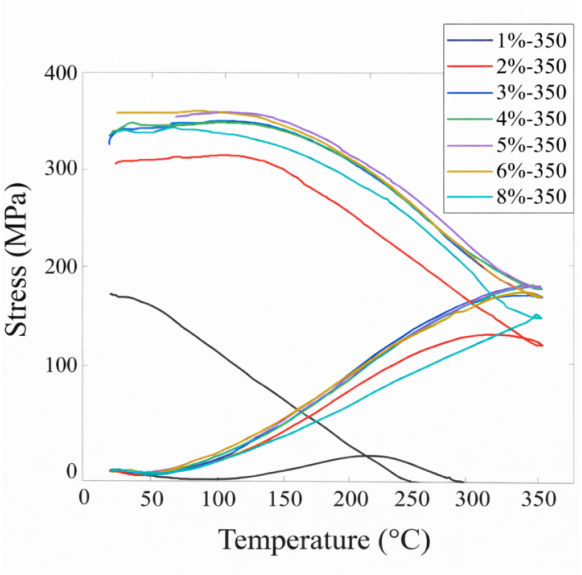

Figure 13. Stress-temperature curves of the V-added Fe-SMAs at different pre-strain levels (recovery at 350℃)

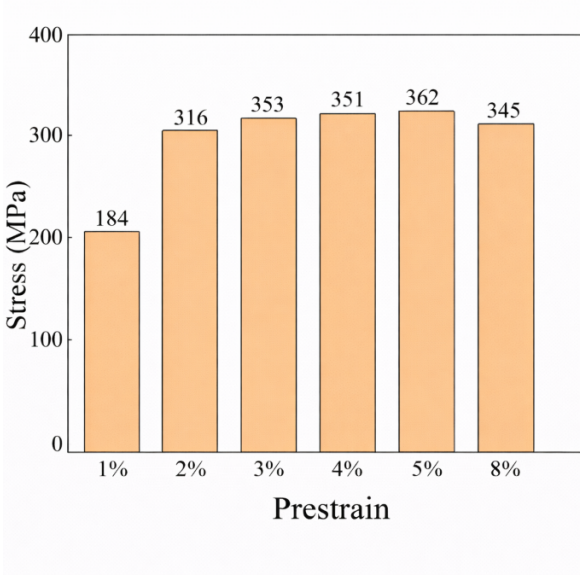

Figure 14. Maximum recovery stress of the V-added Fe-SMAs at different pre-strain levels (recovery at 350℃)

stresses. Martensitic transformation temperature intervals also affect stress recovery during cooling. Thus, tuning this interval via vanadium addition is key to boosting Fe-SMAs' engineering applicability.

3.5 Quantitative Comparison with Existing Research

This study compares the recovery performance of the domestic Fe-SMAs with that of the classic EMPA-developed Fe-17Mn-5Si-10Cr-4Ni-1(V, C) alloy. Under comparable conditions of approximately 5% pre-strain and 350℃ activation temperature, the reported recovery stress for the EMPA alloy ranges between 300–350 MPa [21].

In comparison, the V-added Fe-SMAs from this study achieved a recovery stress of 361.8 MPa , which is slightly higher. The V-free Fe-SMAs produced a stress of 310.6 MPa , falling at the lower end of the reported range for the EMPA alloy. Regarding transformation temperatures, the A_s for the EMPA alloy is approximately 400–450℃. The A_s values for the present V-added and V-free alloys are 432.2℃ and 430.6℃, respectively, both of which fall within

this reasonable interval. These comparisons indicate that the key performance metrics of the domestic Fe-SMAs are comparable to, or in some aspects even surpass, those of their international counterparts. This demonstrates that performance can be further enhanced through compositional optimization.

3.6 Potential Limitations and Future Perspectives for Engineering Application

While the domestic Fe-SMAs show promising potential in mechanical and recovery properties, laying a foundation for their use as active strengthening materials, their path toward mature engineering application still faces systematic challenges [22–26].

Cost is a primary constraint. Although more economical than NiTi alloys [27], the complex melting, rolling processes, and cost of alloying elements make Fe-SMAs more expensive than conventional steel and FRP materials. Widespread application relies on subsequent process optimization and the development of a complete industrial chain [28]. In terms of long-term durability, the performance evolution of the material in corrosive environments and the long-term bond reliability at its interfaces with concrete or steel substrates have not been sufficiently validated. Furthermore, the cyclic loads experienced by actual structures impose higher demands on the fatigue performance of Fe-SMAs. While stress loss during initial cycles and its recoverability upon reheating have been confirmed, the performance degradation mechanisms and long-term prestress retention under variable-amplitude, high-cycle fatigue loading still require in-depth investigation tailored to specific engineering conditions. Environmental adaptability is another concern not to be overlooked. Ambient temperatures below M_f may induce undesired phase transformations, while excessively high temperatures during the activation stage could damage the substrate material. Therefore, developing precise and controllable activation and protection techniques is crucial. In summary, advancing the engineering application of domestic Fe-SMAs requires not only ongoing optimization of material properties and mechanistic studies but also, more critically, the establishment of a regulatory framework including design guidelines and construction standards, coupled with the accumulation of experience from full-scale tests and pilot projects. This integrated approach is essential to bridge the gap between material performance and structural application.

4 Conclusions

This study conducted a systematic investigation into the fundamental mechanical properties and constrained recovery performance of two domestic Fe-Mn-Si shape memory alloys: V-free (Fe-16.86Mn-4.5Si-10.3Cr-5.29Ni-0.08C) and V-added (Fe-17.6Mn-4.5Si-3.22Cr-2.96Ni-0.28C-1.45V). The main conclusions are as follows:

1. Fundamental Mechanical Properties: The V-added Fe-SMAs exhibited superior mechanical properties, with an elastic modulus of 196.7 GPa and a transformation stress of 510.1 MPa, compared to 187.9 GPa and 427.3 MPa for the V-free Fe-SMAs. This indicates that vanadium addition enhances both the stiffness and phase transformation driving capability.

2. The martensitic transformation temperature range of the V-added Fe-SMAs was determined as M_s = 33.9℃ and M_f = -28.8℃, and its austenitic transformation range as A_s = 358.5℃ and A_f = 432.2℃. For the V-free Fe-SMAs, the corresponding temperatures were M_s = 16.5℃, M_f = -1.1℃, A_s = 401.7℃, and A_f = 430.6℃. The addition of vanadium significantly reduced the phase transformation temperature intervals, which is beneficial for temperature control in engineering applications. Furthermore, the average coefficients of thermal expansion within the 30–400℃ range were measured to be 1.33×10^{-5}℃$^{-1}$ and 1.37×10^{-5}℃$^{-1}$ for the V-free and V-added Fe-SMAs, respectively. The close proximity of these values indicates that the addition of vanadium has a limited influence on the thermal expansion behavior.

3. Influence of Activation Temperature: The recovery stress of both Fe-SMAs increased significantly with rising activation temperature. For instance, at 5% pre-strain, the recovery stress of the V-free Fe-SMAs increased from 180.1 MPa at 180℃ to 310.6 MPa at 350℃. The V-added Fe-SMAs yielded even higher recovery stresses under the same conditions, demonstrating stronger recovery capability at identical temperatures due to its lowered transformation temperatures.

4. Influence of Pre-strain Level: The pre-strain level significantly affected the recovery stress, with an optimal value observed. At an activation temperature of 350℃, both the V-free and V-added Fe-SMAs reached their peak recovery stresses (301.8 MPa and 361.8 MPa , respectively) at approximately 6% pre-strain. Beyond this optimal level, the recovery stress gradually decreased due to increased irreversible plastic deformation, highlighting that controlling the pre-strain is key to optimizing Fe-SMAs recovery performance.

In summary, the domestic Fe-SMAs, particularly the V-added variant, demonstrate excellent performance in mechanical properties, transformation control, and recovery characteristics. They possess fundamental engineering applicability as active strengthening materials, providing a significant basis for their potential application in practical bridge strengthening projects.

Author Contributions

Conceptualization, H.L.M. and Y.F.Z.; methodology, H.L.M.; software, H.L.M.; validation, H.L.M. and Y.F.Z.; formal analysis, H.L.M.; investigation, H.L.M.; resources, H.L.M.; data curation, H.L.M.; writing-original draft preparation, H.L.M.; writing—review and editing, H.L.M. and Y.F.Z.; visualization, H.L.M.; supervision, Y.F.Z.; project administration, Y.F.Z.; funding acquisition, Y.F.Z. All authors have read and agreed to the published version of the manuscript.

Funding

This work is funded by the Fundamental Research Funds for the Central Universities (Grant No.: 419080600283).

Data Availability

The data used to support the research findings are available from the corresponding author upon request.

Conflicts of Interest

The authors declare no conflict of interest.

References

[1] Q. Quan, "Health monitoring of bridge structures," *China J. Highw. Transp.*, no. 2, pp. 39–44, 2000. https://doi.org/10.19721/j.cnki.1001-7372.2000.02.010

[2] J. A. O. Barros, D. R. S. M. Ferreira, A. S. Fortes, and S. J. E. Dias, "Assessing the effectiveness of embedding CFRP laminates in the near surface for structural strengthening," *Constr. Build. Mater.*, vol. 20, no. 7, pp. 478–491, 2006. https://doi.org/10.1016/j.conbuildmat.2005.01.030

[3] Q. Jia, "Diseases and reinforcement methods of road and bridge structures," *Commun. Sci. Technol. Heilongjiang*, vol. 34, no. 10, p. 265, 2011. https://doi.org/10.16402/j.cnki.issn1008-3383.2011.10.204

[4] C. E. Bakis, L. C. Bank, V. L. Brown, E. Cosenza, J. F. Davalos, J. J. Lesko, A. Machida, S. H. Rizkalla, and T. C. Triantafillou, "Fiber-reinforced polymer composites for construction—State-of-the-art review," *J. Compos. Constr.*, vol. 6, no. 2, pp. 73–87, 2002. https://doi.org/10.1061/(ASCE)1090-0268(2002)6:2(73)

[5] M. I. Kabir, "Short and long term performance of concrete structures repaired/strengthened with FRP," Ph.D. dissertation, University of Technology Sydney, Australia, 2014.

[6] H. Toutanji and G. Ortiz, "The effect of surface preparation on the bond interface between FRP sheets and concrete members," *Compos. Struct.*, vol. 53, no. 4, pp. 457–462, 2001. https://doi.org/10.1016/S0263-8223(01)00057-5

[7] C. Mazzotti, M. Savoia, and B. Ferracuti, "A new single-shear set-up for stable debonding of FRP-concrete joints," *Constr. Build. Mater.*, vol. 23, no. 4, pp. 1529–1537, 2009. https://doi.org/10.1016/j.conbuildmat.2008.04.003

[8] S. Kueres, N. Will, and J. Hegger, "Shear strength of prestressed FRP reinforced concrete beams with shear reinforcement," *Eng. Struct.*, vol. 206, p. 110088, 2020. https://doi.org/10.1016/j.engstruct.2019.110088

[9] G. Şakar and H. M. Tanarslan, "Prestressed CFRP fabrics for flexural strengthening of concrete beams with an easy prestressing technique," *Mech. Compos. Mater.*, vol. 50, no. 4, pp. 537–542, 2014. https://doi.org/10.1007/s11029-014-9440-0

[10] W. W. Wang, J. G. Dai, K. A. Harries, and Q. H. Bao, "Prestress losses and flexural behavior of reinforced concrete beams strengthened with posttensioned CFRP sheets," *J. Compos. Constr.*, vol. 16, no. 2, pp. 207–216, 2012. https://doi.org/10.1061/(ASCE)CC.1943-5614.0000255

[11] J. Michels, J. Sena-Cruz, C. Czaderski, and M. Motavalli, "Structural strengthening with prestressed CFRP strips with gradient anchorage," *J. Compos. Constr.*, vol. 17, no. 5, pp. 651–661, 2013. https://doi.org/10.1061/(ASCE)CC.1943-5614.0000372

[12] L. A. Montoya-Coronado, J. G. Ruiz-Pinilla, C. Ribas, and A. Cladera, "Experimental study on shear strengthening of shear critical RC beams using iron-based shape memory alloy strips," *Eng. Struct.*, vol. 200, p. 109680, 2019. https://doi.org/10.1016/j.engstruct.2019.109680

[13] A. Cladera, L. A. Montoya-Coronado, J. G. Ruiz-Pinilla, and C. Ribas, "Shear strengthening of slender reinforced concrete T-shaped beams using iron-based shape memory alloy strips," *Eng. Struct.*, vol. 221, p. 111018, 2020. https://doi.org/10.1016/j.engstruct.2020.111018

[14] Z. Liu, H. Zhu, Y. Zeng, Z. Dong, J. Ji, G. Wu, and X. Zhao, "Study on the flexural properties of T-shaped concrete beams reinforced with iron-based shape memory alloy rebar," *Eng. Struct.*, vol. 306, p. 117792, 2024. https://doi.org/10.1016/j.engstruct.2024.117792

[15] M. Shahverdi, C. Czaderski, P. Annen, and M. Motavalli, "Strengthening of RC beams by iron-based shape memory alloy bars embedded in a shotcrete layer," *Eng. Struct.*, vol. 117, pp. 263–273, 2016. https://doi.org/10.1016/j.engstruct.2016.03.023

[16] R. El-Hacha and K. Soudki, "Prestressed near-surface mounted fibre reinforced polymer reinforcement for concrete structures – A review," *Can. J. Civ. Eng.*, vol. 40, no. 11, pp. 1127–1139, 2013. https://doi.org/10.1139/cjce-2013-0063

[17] C. Cui, Z. Dong, H. Zhu, Y. Zhao, T. Han, Y. Pan, and E. Ghafoori, "Axial compressive behavior of UHPC columns reinforced with self-prestressed Fe-SMA spiral stirrups," *Structure*, vol. 77, p. 109107, 2025. https://doi.org/10.1016/j.istruc.2025.109107

[18] W. J. Lee, B. Weber, G. Feltrin, C. Czaderski, M. Motavalli, and C. Leinenbach, "Phase transformation behavior under uniaxial deformation of an Fe-Mn-Si-Cr-Ni-VC shape memory alloy," *Mater. Sci. Eng. A*, vol. 581, pp. 1–7, 2013. https://doi.org/10.1016/j.msea.2013.06.002

[19] P. Feng, H. L. Qiang, and L. P. Ye, "Discussion and definition on yield points of materials, members and structures," *Eng. Mech.*, vol. 34, no. 3, pp. 36–46, 2017. https://doi.org/10.6052/j.issn.1000-4750.2016.03.0192

[20] E. Patoor and M. Berveiller, *Technologie Des Alliages À MÉMoire De Forme: Comportement MÉCanique Et Mise En Œuvre*. Hermés science, 1994.

[21] M. Shahverdi, J. Michels, C. Czaderski, and M. Motavalli, "Iron-based shape memory alloy strips for strengthening RC members: Material behavior and characterization," *Constr. Build. Mater.*, vol. 173, pp. 586–599, 2018. https://doi.org/10.1016/j.conbuildmat.2018.04.057

[22] Y. C. Gong, C. X. Qu, T. H. Yi, L. Ren, J. Zhang, and H. N. Li, "A theoretical analysis method of transverse modal shapes of hollow slab bridge with hinge joint damage," *Structure*, vol. 56, p. 104832, 2023. https://doi.org/10.1016/j.istruc.2023.07.022

[23] W. Wang, L. Li, A. Hosseini, and E. Ghafoori, "Novel fatigue strengthening solution for metallic structures using adhesively bonded Fe-SMA strips: A proof of concept study," *Int. J. Fatigue*, vol. 148, p. 106237, 2021. https://doi.org/10.1016/j.ijfatigue.2021.106237

[24] W. Wang, A. Hosseini, and E. Ghafoori, "Experimental study on Fe-SMA-to-steel adhesively bonded interfaces using DIC," *Eng. Fract. Mech.*, vol. 244, p. 107553, 2021. https://doi.org/10.1016/j.engfracmech.2021.107553

[25] S. Wang, L. Li, Q. Su, X. Jiang, and E. Ghafoori, "Strengthening of steel beams with adhesively bonded memory-steel strips," *Thin-Walled Struct.*, vol. 189, p. 110901, 2023. https://doi.org/10.1016/j.tws.2023.110901

[26] L. Li, E. Chatzi, and E. Ghafoori, "Debonding model for nonlinear Fe-SMA strips bonded with nonlinear adhesives," *Eng. Fract. Mech.*, vol. 282, p. 109201, 2023. https://doi.org/10.1016/j.engfracmech.2023.109201

[27] A. Cladera, B. Weber, C. Leinenbach, C. Czaderski, M. Shahverdi, and M. Motavalli, "Iron-based shape memory alloys for civil engineering structures: An overview," *Constr. Build. Mater.*, vol. 63, pp. 281–293, 2014. https://doi.org/10.1016/j.conbuildmat.2014.04.032

[28] T. Maruyama and H. Kubo, "Ferrous (Fe-based) shape memory alloys (SMAs): Properties, processing and applications," in *Shape Memory and Superelastic Alloys: Technologies and Applications*. Woodhead Publishing, 2011, pp. 141–159.